2018

Modeling the Impacts of Sea Level Rise on Storm Surge Inundation in Flood-Prone Urban Areas of Hampton Roads, Virginia

Luca Castrucci
Old Dominion University, lcast012@odu.edu

Navid Tahvildari
Old Dominion University, ntahvild@odu.edu

Repository Citation

Castrucci, Luca and Tahvildari, Navid, "Modeling the Impacts of Sea Level Rise on Storm Surge Inundation in Flood-Prone Urban Areas of Hampton Roads, Virginia" (2018). *Civil & Environmental Engineering Faculty Publications*. 27.
https://digitalcommons.odu.edu/cee_fac_pubs/27

Original Publication Citation

Castrucci, L. and Tahvildari, N. (2018). Modeling the impacts of sea level rise on storm surge inundation in flood-prone urban areas of Hampton Roads, Virginia. *Marine Technology Society Journal, 52*(2), 92-105. doi: 10.4031/MTSJ.52.2.11

PAPER

Modeling the Impacts of Sea Level Rise on Storm Surge Inundation in Flood-Prone Urban Areas of Hampton Roads, Virginia

AUTHORS
Luca Castrucci
Navid Tahvildari
Department of Civil and
Environmental Engineering,
Old Dominion University

ABSTRACT

Hampton Roads is a populated area in the United States Mid-Atlantic region that is highly affected by sea level rise (SLR). The transportation infrastructure in the region is increasingly disrupted by storm surge and even minor flooding events. The purpose of this study is to improve our understanding of SLR impacts on storm surge flooding in the region. We develop a hydrodynamic model to study the vulnerability of several critical flood-prone neighborhoods to storm surge flooding under several SLR projections. The hydrodynamic model is validated for tide prediction, and its performance in storm surge simulation is validated with the water level data from Hurricane Irene (2011). The developed model is then applied to three urban flooding hotspots located in Norfolk, Chesapeake, and the Isle of Wight. The extent, intensity, and duration of storm surge inundation under different SLR scenarios are estimated. Furthermore, the difference between the extent of flooding as predicted by the hydrodynamic model and the “bathtub” approach is highlighted.

Keywords: hydrodynamic modeling, storm surge, sea level rise, flooding of transportation infrastructure

Introduction

Nearly 30% of the U.S. population, or 87.4 million people, lived in coastal counties in 2008, showing an increase of 84.3% with respect to 1960 (Wilson & Fischetti, 2010). Recent hurricanes Irma (2017), Harvey (2017), Sandy (2012), and Katrina (2005) have had devastating impacts on highly populated coastal areas in the U.S. Gulf and Atlantic Coasts. High wind speed and storm surge flooding are the main hazards for people and coastal infrastructure. Prior to major storms, the authorities may demand evacuation of residents from areas vulnerable to storm surge. State roads and interstates prove to be the preferred evacuation routes, despite the potential high vulnerability that they may have in respect to flooding (Kleinosky et al., 2007).

Climate change and its consequences, including sea level rise (SLR), threaten the low-lying coastal infrastructure, and hence, accurate estimation of storm surge flooding in the current and future state of the climate is critical for coastal planning and management. SLR provides a path for storm surge and energetic oceanic waves to propagate toward the infrastructure in the upland and cause damage. Furthermore, atmospheric models suggest that climate change can result in an increase in the number of large hurricanes (Bender et al., 2010).

Storm surge flooding may be estimated using different approaches depending on the necessities and the resources available (Murdukhayeva et al., 2013). For instance, the “bathtub” approach has long been used to estimate the extent of storm surge flooding and SLR impacts. Although this approach can provide first-order estimates of storm surge, it can include significant inaccuracies since it is based on static increase in water level. However, the response of storm surge to increase in sea level is nonlinear, such that a certain amount of increase in sea level does not necessarily result in the same amount of increase in storm surge flooding (Atkinson et al., 2013). This is due to the complex physics of the interactions among storm surge, tides, waves, and the overland flow, as well as their interactions with the natural and urbanized landscape. Therefore, a more accurate estimate of storm surge requires an approach that accounts for the dynamicity of storm and tides.

The Hampton Roads region of Virginia is one of the most vulnerable areas in the world to climate change and SLR in terms of population size and values of assets. It is a metropolitan region located at the confluence of the James, Elizabeth, and Nansemond rivers and comprises 10 cities with a total population of 1.7 million. The Port of Virginia located at Hampton Roads is the second largest port on the East Coast of the United States, and Norfolk is home to the largest naval base in the world. The region has the second highest relative SLR rate in the United States (~7 mm/year) only behind New Orleans (Boon et al., 2010). Several factors including crustal warping, sediment compaction, and groundwater withdrawal (Kleinosky et al., 2007), as well as the dynamics of the Gulf Stream (e.g., Ezer et al., 2013), contribute to this high rate of relative SLR. Recurrent flooding of the infrastructure is a common occurrence in the region, and SLR has exacerbated the problem. Research shows that the accelerated rate of minor flooding due to high tides and precipitation in recent years can be attributed to SLR (Ezer & Atkinson, 2014).

Several previous studies have investigated storm surge flooding in the Hampton Roads region. For instance, Li et al. (2013) used the Coastal Modeling System (CMS), a suite of models that simulate storm surge, waves, circulation, sediment transport, and morphological change, to study SLR impacts on Naval Station Norfolk. The domain of the CMS was limited to the naval base, and the boundary conditions to this domain were produced by the ADCIRC model (Westerink et al., 2008). Loftis et al. (2016) used the subgrid modeling approach (Neelz & Pender, 2007) to simulate the precipitation- and storm surge-driven flooding in NASA Langley Research Center. The approach allows for nesting high-resolution LiDAR elevation data in lower-resolution computational grids of the hydrodynamic model. They show that flooding estimation improves by accounting for infiltration using land use data. The hydrodynamic model used in the study is the UnTRIM^2 model (Casulli & Stelling, 2011). Sadler et al. (2017) estimated the most vulnerable transportation infrastructure is in the Hampton Roads cities of Norfolk and Virginia Beach. Applying the "bathtub" approach, results suggested that under the intermediate scenario, by 2100 around 10% of major roads in Virginia Beach and Norfolk were predicted to regularly flood due to tides reaching 2.1 m NAVD88. The percentage increases to over 15% of major roads with a 99% tide (2.6 m) and to over 65% of major roads with the addition of a 100-year storm surge (4.5 m). The study uses the "bathtub" approach to add storm surge estimates to SLR projections. Consequently, earlier flooding studies have either used the "bathtub" approach (e.g., Sadler et al., 2017) or have used hydrodynamic models to focus on a small study area (Li et al., 2013; Loftis et al., 2016).

In this study, a hydrodynamic model is developed to predict hurricane storm surge in high resolution at several flood-prone critical spots in the Hampton Roads region of Virginia. These critical spots are known to experience recurrent and storm surge flooding that causes disruption in the transportation infrastructure. This study expands the earlier investigation by Castrucci and Tahvildari (2017) in which the vulnerability of two critical areas in Norfolk to storm surge flooding was assessed. The effect of various SLR projections on storm surge flooding is considered.

Methodology

The hydrodynamic model of the region is developed based on the Delft3D model. Delft3D is a widely used three-dimensional modeling suite that can simulate coastal, estuarine, and riverine processes. The model has recently been used for storm surge simulations (Vatvani et al., 2012; Hu et al., 2015). The hydrodynamic model is set up with boundary conditions at the bottom (bathymetry and topography), water surface (atmospheric forcing), tidal forcing, and freshwater input at the boundaries. The model then solves the complex interactions between the flow and the landscape over a computational grid and obtains high temporal and spatial resolution information on water surface elevation at grid cell centers and flow velocity at grid cell faces.

The wind field that drives the storm surge is generated using the Holland et al. (2010) parametric model and the pressure and track data for Hurricane Irene (2011) provided by the National Oceanic and Atmospheric Administration (NOAA) National Hurricane Center (Lixion & Cangialosi, 2011). We assess the impacts of three SLR scenarios, namely intermediate-low (IL), intermediate-high (IH), and extreme on storm surge flooding of three flood-prone critical spots. These areas are the West Brambleton Avenue (US 58) and the Hague neighborhood in the City of Norfolk, the James River Bridge that connects Isle of Wight County to the City of Newport News, and the High Rise Bridge on I-64 in the City of Chesapeake. The first spot was selected due to historic issues with recurrent flooding and vicinity to the Norfolk General Hospital, which houses the region's only Level 1 trauma center (Scott Smith [City of Norfolk], personal communication). The last two spots were selected due to known flooding problems and substantial traffic volume (Robert Morgan & Andrew Scott [Virginia Department of Transportation], personal communication). By comparing model output on water levels with high-resolution topographic data obtained from a geographic information system data set, we determine the flooding extent, intensity, and duration at these critical points. Accurate prediction of the time and duration of flooding at these areas will help the decision makers with advanced warnings and rerouting of the general traffic as well as emergency vehicles.

Hydrodynamic Model Setup

In this study, we use the Delft3D-FLOW model to simulate the nonsteady flow processes generated by tidal and meteorological forcing. The model solves the equations for fluid motion and obtains flow variables, namely velocity vectors, pressure, and water surface elevations over a computational grid.

Grid Generation

The grid size is selected such that the results are obtained at high spatial resolution while keeping the computational time reasonable. It is noted that, in a grid with a variety of cell sizes, the simulation time step is governed by the smallest cell. Therefore, an efficient way to run the simulations using structured grids is to define multiple models with different domain extents that have nearly uniform grid cell sizes. In this approach, known as model nesting, the model that covers a larger geographical area will have a lower grid resolution (Level 1) and produces the boundary condition for a nested model (Level 2) that has a computational grid covering an area within the larger grid of the model at Level 1. The nesting can continue to higher levels (e.g., Levels 3, 4, etc.) in a similar manner. An advantage of model nesting approach is that it allows for utilizing high-resolution data (e.g., meteorological, topographic, or bathymetric data) at higher levels of nesting where high-resolution output is desired whereas low-resolution data are used at the models in lower levels of nesting. This approach will result in considerable reduction in computational time. In this study, we decided to develop the hydrodynamic models in three levels of nesting (Levels 1–3). This approach allows us to use high-resolution LiDAR data (0.76 m horizontal resolution) at several critical flood-prone spots in Level 3 models and keep the computational time reasonable with available resources.

The computational grid of the Level 1 model is shown in Figure 1. The grid is equidistant, such that the distances between a cell center and adjacent cell centers are equal. The cell size in this grid is 125 × 200 m^2. Figure 2 shows the computational grid of the Level 2 model as well as grids of local Level 3 models. The grids of Level 2 and Level 3 models are curvilinear, and their cell sizes vary 30–90 × 30–90 m^2 and 2.5–3.5 × 2.5–3.5 m^2, respectively. The yellow lines in Figure 2 show the boundaries of the Level 2 model, and red areas show the domain of high-resolution Level 3 models, which are constructed around the critical spots. The high grid resolution in Level 3 models enables us to utilize

FIGURE 1

(a) Delft3D model domain at Level 1 of nesting and (b) the computational grid of the Level 1 model in the Hague neighborhood in Norfolk.

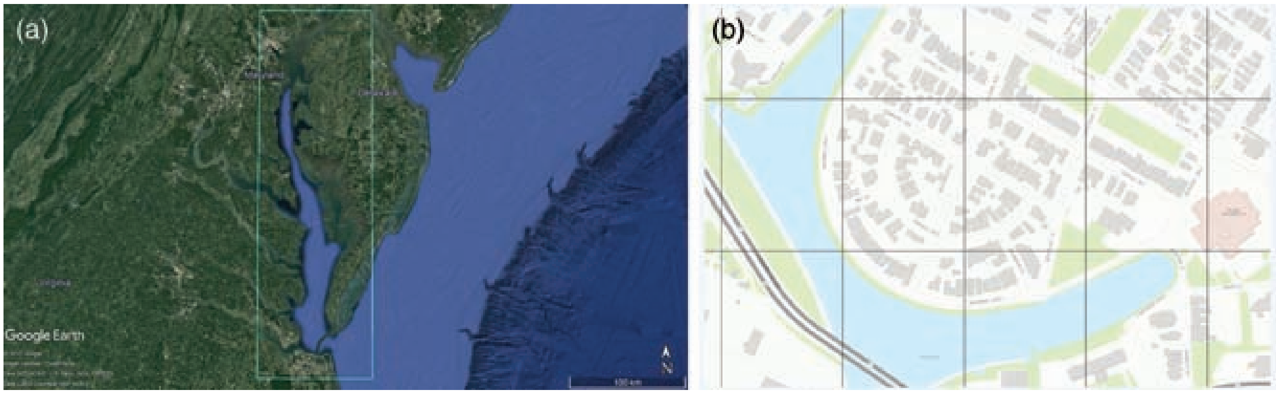

FIGURE 2

(a) Level 2 (specified in yellow) and Level 3 (specified in red) model domains, (b) the computational grid of the Level 2 model, and (c) Level 3 models in the Hague neighborhood in Norfolk.

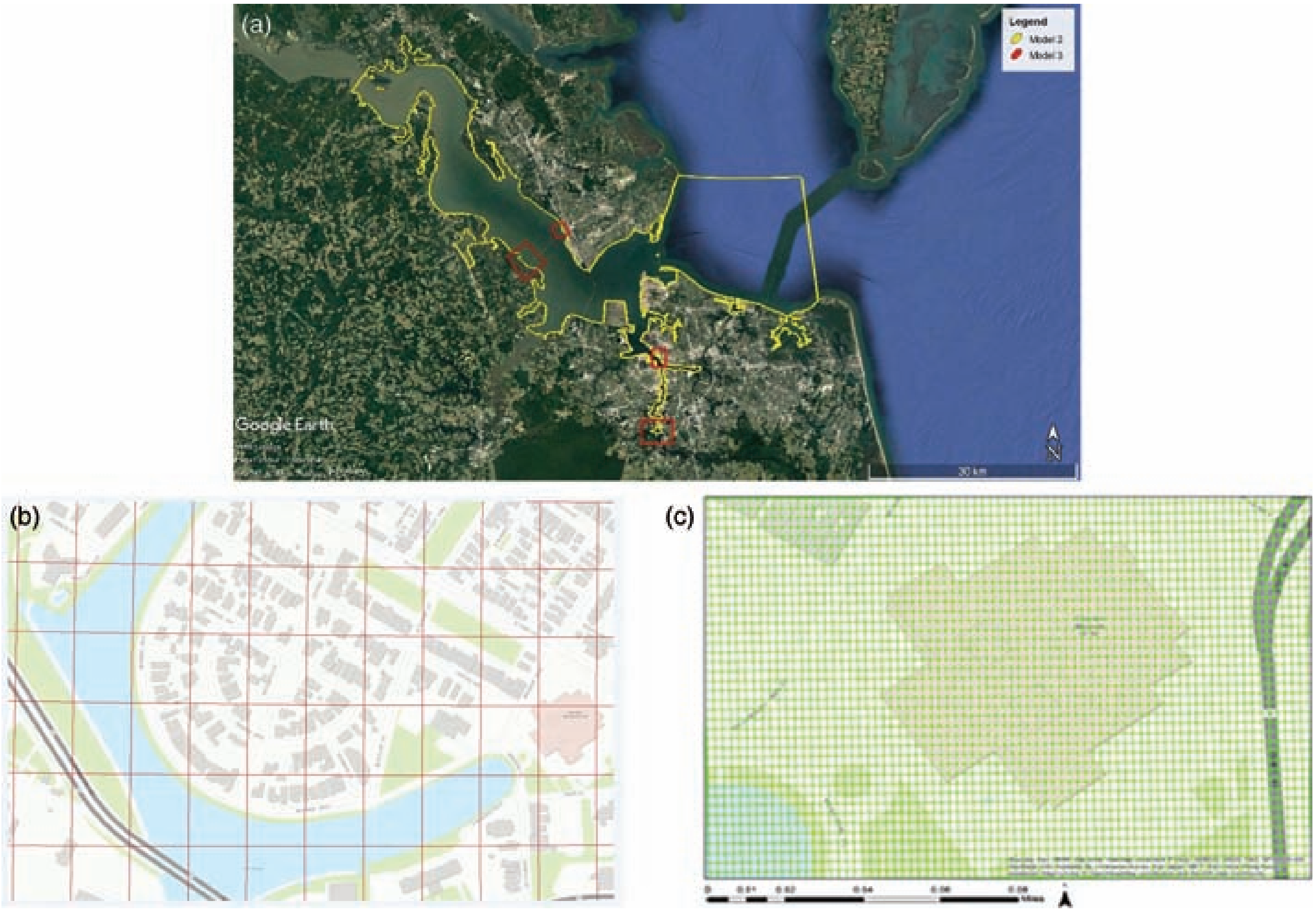

high-resolution LiDAR data and develop street level flood maps.

Boundary Conditions

The hydrodynamic storm surge model requires topography, bathymetry, tide, wind, and river discharge data to perform the numerical simulations.

Topography and Bathymetry Data. The accuracy of the predictions of hydrodynamic models depends on the resolution of the available data (Sebastian et al., 2014). High-resolution LiDAR topographic data for this project are not available for the entire Hampton Roads region, but it completely covers the cities of Norfolk, Hampton, Virginia Beach, and Chesapeake. The topographic data were extracted from the digital elevation model of this data set, which has a 0.76 m horizontal resolution and was utilized in the simulations that used the Level 3 model. In Level 1 and Level 2 models, which have larger domains, we used the freely available highest-resolution bathymetric and topographic data from NOAA. Table 1 summarizes the sources of the topographic/bathymetric data used in the

TABLE 1

The bathymetric and topographic data sources and resolution in the nested model.

Data	Source	Resolution/Nesting Level
Topography	NOAA–Coastal Relief Model	90 m/first level
Topography	NOAA–Virginia Beach Raster	10–30 m/second level
Topography	USGS–Hampton Roads LiDAR	0.76 m/third level
Bathymetry	NOAA–Coastal Relief Model	90 m/first level
Bathymetry	NOAA–Virginia Beach Raster	10–30 m/second and third level

study as well as the spatial resolution of each data set. The elevation data from different sources did not have the same datum and coordinate system, and as such, they were converted to NAVD 88 using VDatum. Although the bathymetry and topography had the same resolution in Level 1 and Level 2 models, their resolution differed in Model 3 where the topography and bathymetry had 0.76 m and 10–30 m resolution, respectively.

Tides. High tides contribute to the flooding significantly, and they should be accounted for in the storm surge model. The Delft3D model is forced by amplitudes and phases of nine primary tidal constituents (M_2, S_2, N_2, K_2, K_1, O_1, P_1, Q_1, and M_4) at the open boundaries of the Level 1 model. The amplitudes and the phases of these harmonics were interpolated using the values from the TPXO global tide model (Egbert & Erofeeva, 2002), which has a 1/30° resolution at the U.S. East Coast. The points where the tidal information is extracted are selected such that they are close to the coastline, otherwise the tidal propagation in shallow water may not be adequately reproduced due to relatively low topography and bathymetry resolution in the Level 1 model.

Wind Profile. The most important boundary condition in hurricane surge simulation is the wind and pressure fields. According to the data from the NOAA tide gauge at Sewells Point, VA, Hurricanes Irene (2011) and Sandy (2012) caused the largest storm surge among the hurricanes that affected the Hampton Roads region in the past decade. The storm surge that resulted from these two hurricanes in Hampton Roads (based on measurements at the Sewells Point tide gauge) are nearly the same. For this research we decided to use the characteristics of Hurricane Irene to set up the wind field. Because of the low resolution of wind and pressure data from satellites, the hurricane profile was created using the Holland et al. (2010) model. The model generates the wind profile using the maximum wind velocity, minimum pressure, and storm diameter. The storm path, maximum wind velocity, and minimum pressure were provided by the NOAA National Hurricane Center (Lixion & Cangialosi, 2011), whereas the storm diameter was estimated according to the Gross et al. (2004) model. The output values from the Holland et al. (2010) model were inserted in a meteo mesh, which shaped as a spider web can host variable grid sizes that increase resolution as they approach the center of the network. The spider web grid was generated to be large enough to accommodate changes in storm size, which varies with maximum velocity and central pressure, which experienced changes along Hurricane Irene's path. The main characteristic of the spider web domain is related to its nonstationary position, which changes during the simulation according to the hurricane path. The wind field is interpolated to the computational grid.

River Discharge. The discharge of the James River is used as a boundary condition in the western open boundary of the Level 2 model. The river discharge is recorded every quarter of an hour by a United States Geological Survey (USGS) gauge located near Richmond, Virginia.

Results

Model Validation

Prior to applying the storm surge model to future SLR scenarios, we validate the model with the observed storm surge from Hurricane Irene (2011). The validated storm surge model then uses the Hurricane Irene parameters to predict storm surge levels and flooding duration due to Irene-like storms in future sea level conditions.

The model parameters are kept constant over the three levels of nesting. Sea water density is 1,025 kg/m^3, background atmospheric pressure is 1,030 mbar, the bottom roughness is represented by the Manning coefficient, which is assumed to be 0.03 in the Level 1 model and 0.02 in both Level 2 and Level 3 models. These values were obtained through tide calibration. Horizontal eddy viscosity is kept the same as the default value of 1 m^2/s. All the boundary conditions in the model, such as bathymetry and initial water level, have been specified at the corners of the grid cells, and the threshold depth for wetting and drying is specified to be 0.1 m. The vertical datum is NAVD88. We used the data from two NOAA tide gauges located at the Chesapeake Bay Bridge Tunnel (CBBT) and the Sewells Point to validate the performance of the Delft3D model. The CBBT data were used to validate the Level 1 model. The domain extent and grid resolution of the Level 1 model were selected such that the storm track through the Hampton Roads area is captured adequately while ensuring that the grid has a high enough resolution to capture the storm and tide propagation into the Chesapeake Bay. As seen in Figure 3(a), Level 1 model results for Hurricane Irene and the tidal elevations prior to the storm compare well with the buoy data. The root mean square error (RMSE) is 0.156 m. The only notable discrepancy occurs

FIGURE 3

Comparison between hydrodynamic model results for water level and measurements at (a) CBBT and (b) Sewells Point tide gauges during Hurricane Irene (2011).

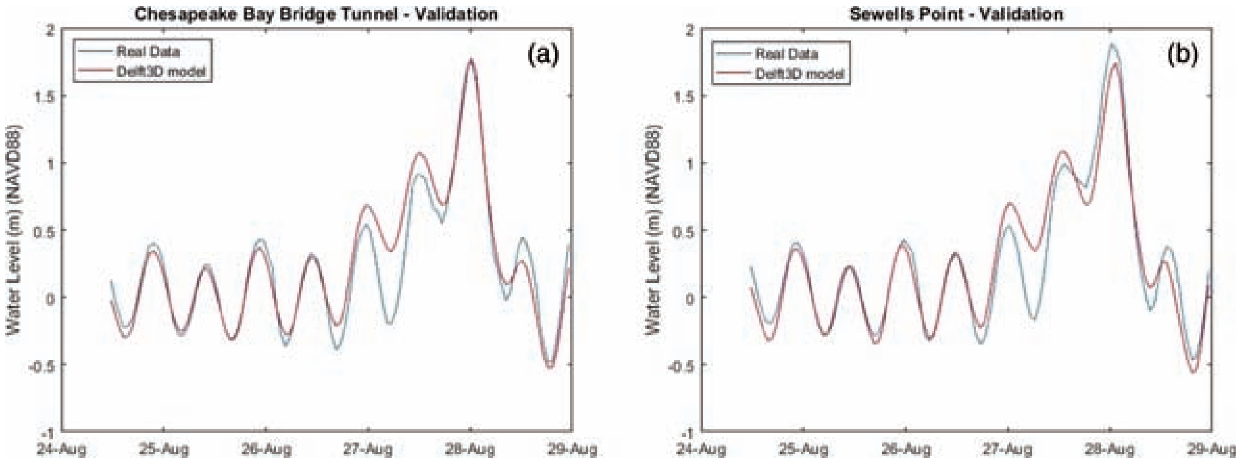

at two tidal cycles prior to the storm peak, which can be due to uncertainty in the size of the storm in this time frame; Hurricane Irene's radius was hard to estimate due to larger than normal size of the cyclone and the absence of a particularly intense inner core during August 26–27 (Lixion & Cangialosi, 2011). Therefore, we hypothesize that the assumption that the hurricane radius is constant with time and space may have resulted in this discrepancy. We note that the HWind legacy data for Hurricane Irene is publicly available and using the data may resolve these discrepancies. However, recent research shows that a hydrodynamic + wave model that uses a Holland-type parameterization for atmospheric forcing can provide a more accurate estimation of storm surge than the model, which uses HWind data (Dietrich et al., 2017). The study used the data from Hurricane Isaac (2012) in the Gulf of Mexico, and the results of the study may not be applicable to the present investigation. Nevertheless, the model estimation for water levels at the storm peak compare well with the data. Level 2 model is validated using the Sewells Point tide gauge. As seen in Figure 3(b), the model result for tidal elevation and the storm surge compare well with the data. The RMSE is 0.155 m. The slight discrepancy observed at the peak may be attributed to the inadequacy in representation of the shallow bathymetry in the model. There were no tide gauges in the domains of Level 3 models in 2011; hence, the calibration and validation of these models with tide and storm surge data were not possible. However, a tide gauge was installed on a bridge in the Hague area in 2016, and the data can be used for similar future studies.

Storm Surge Under SLR

Several critical flood-prone locations were considered, and three were selected for this study: the Hague neighborhood located in downtown Norfolk, the James River Bridge connecting the Isle of Wight county to the City of Newport News, and the I-64 Bridge in Chesapeake. These three spots are known to be vulnerable to direct storm surge inundation, and their flooding can significantly disrupt the traffic flow. It is worth noting that there are many spots in the transportation infrastructure in the region that are indirectly vulnerable to storm surge flooding. In these spots, higher water due to storm surge and high tides submerge the outlets and cause the storm water to back up in the drainage system and prevent the storm water infrastructure from functioning properly. This effect will contribute to flooding even in areas that are not directly inundated by storm surge. However, our study is focused on the direct storm surge-induced inundation.

We considered three SLR projections presented in a recent NOAA report by Sweet et al. (2017). This report adds an extreme flooding scenario to estimates proposed in earlier studies. In this study, we use SLR with IL, IH, and extreme rates. Table 2 summarizes these estimates for 2050 and 2100, the two time frames considered in this study. It should be noted that the study can readily be extended to other SLR estimates. The effect of SLR is added to the model by increasing the water level to the desired values at the boundaries of Model 1

TABLE 2

SLR scenarios used in storm surge simulations. These values are obtained from Sweet et al. (2017).

SLR (m)	2050	2100
IL	0.24	0.5
IH	0.44	1.5
Extreme	0.63	2.5

FIGURE 4

Flood map at the Hague neighborhood for Irene-like hurricanes under IL, IH, and extreme SLR in (a) 2050 and (b) 2100. The blue pin shows the locations where the model outputs flooding level and duration.

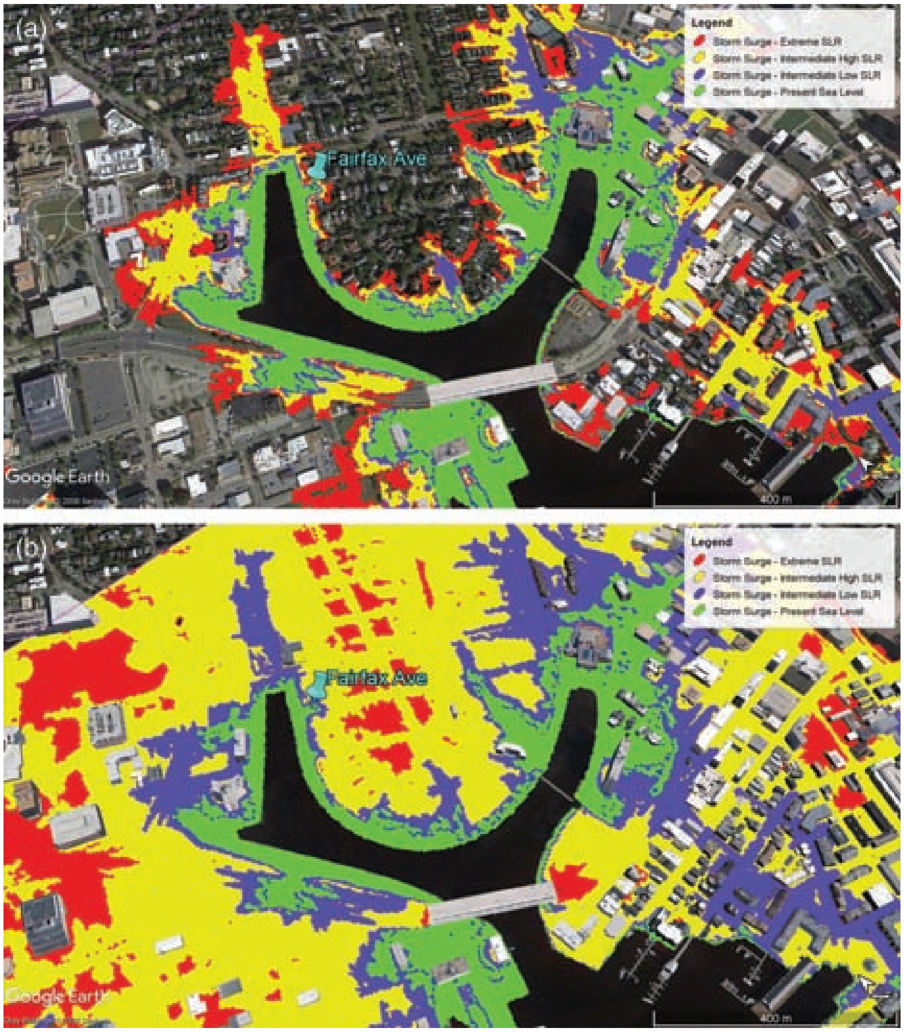

and allows enough time for the sea level change to propagate throughout the domain. This will change the boundary conditions for Models 2 and 3 subsequently.

In Figure 4, the extent of storm surge flooding in the Hague area is depicted. The map shows the extent of flooding due to Hurricane Irene (2011) under the present sea level as well as potential hurricanes that could occur in 2050 with the same parameters as Hurricane Irene under SLR projections outlined in Table 2. As expected, flooded areas increase with increase in SLR projection for the year 2050. In the year 2100, the extent of inundation is significantly increased from IL to IH scenario, such that a wide area of the city, well beyond the Hague area, will be inundated. The increase in flooding extent from IH to the extreme SLR scenario is not as pronounced. Note the upland border of the computational grid in Figure 4(b) indicating that areas that are not colored in this figure are outside the grid and not necessarily dry.

In addition to depth of water level over the flooded area, the hydrodynamic modeling approach allows us to estimate the duration of flooding. In estimating the flooding duration, we assumed that a location is flooded once the total water level (storm surge + tide + SLR) is higher than the elevation of the point. It should be noted that the hydrodynamic model does not account for drainage, infiltration, or evaporation, and hence, if the water creates a pond at a low-lying spot after the storm surge has receded, the water level will remain at a constant nonzero value at that location. Therefore, we considered flooding to end once the water level is subsided and reaches a value that is constant with time, even if this value is not zero. It is noted that the 0.10 m threshold for wetting/drying filters out some of the ponds, but in some of the simulations, the depth of the ponds saturated to a value larger than this threshold after the completion of the storm.

Flood level, defined as the maximum water surface elevation during the storm event, and *flood duration,* defined as the time over which the model predicts the existence of water over an area, are the two main outputs of the model. The "observation point," where this information is output at high temporal resolution, is

FIGURE 5

Storm surge flooding intensity (a) and duration (b) at the Hague area in Norfolk, VA, due to Hurricane Irene under present sea level and IL, IH, and extreme scenarios.

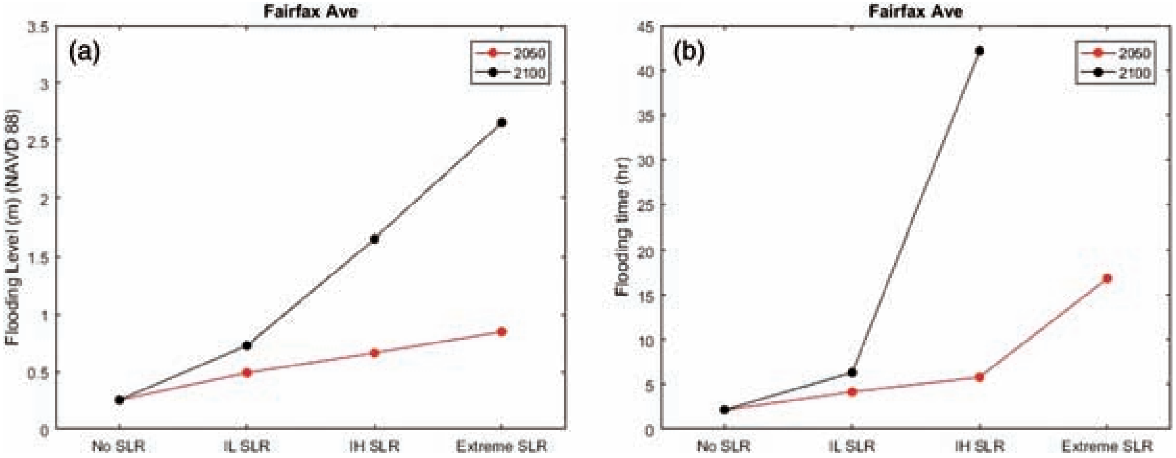

shown by a blue pin in Figure 4. In the Hague area, we placed the observation point at the Fairfax Avenue as a representative spot in the area. As seen in Figure 5, flooding level increases linearly with SLR scenarios in 2050. On the other hand, the flooding level in 2100 and flooding time increase nonlinearly with SLR scenarios. It is also noted that the trend in flooding times shows a significant increase from the IL to IH

FIGURE 6

Flood maps for the north (a, b) and south (c, d) sides of the James River Bridge in 2050 and 2100. SLR scenarios include IL, IH, and extreme conditions.

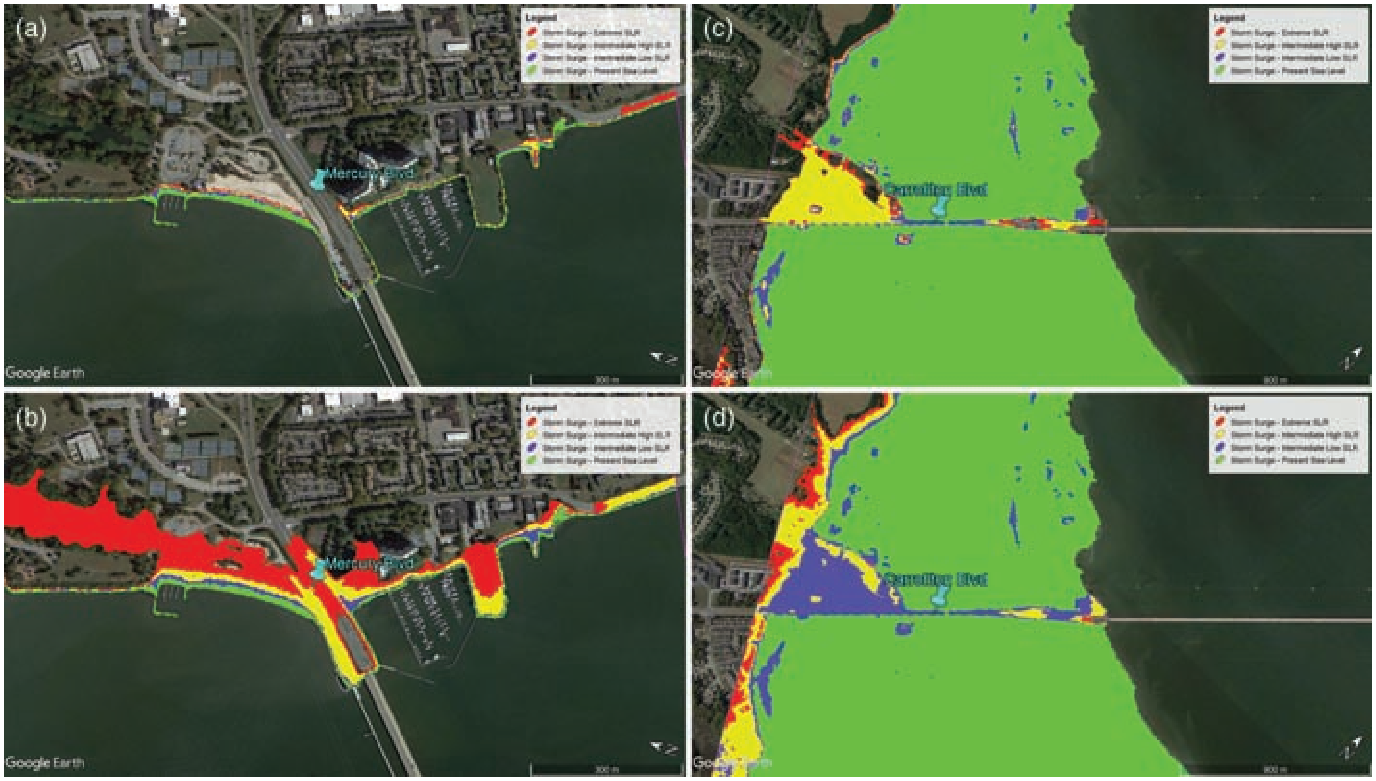

scenario in 2100, whereas the difference between current sea level condition and IH scenario is not as pronounced. The neighborhood is under water in extreme SLR scenarios at 2100 even without storm surge; thus, the flooding time for this scenario is not included in Figure 5(b).

The second critical spot in this study is the bridge over James River, which connects Isle of Wight County to Newport News and has a high traffic volume. Castrucci and Tahvildari (2017) showed that the north side of the bridge is not vulnerable to storm unless IH or extreme SLR conditions are considered. In this study, we extend the analysis to include a spot in the south side of the bridge, which has a significantly lower elevation than the north side, and hence will determine the storm surge and SLR conditions that will disrupt traffic flow through the bridge. Figure 6 shows flood maps at the north (Mercury Blvd.) and south (Carrolton Blvd.) side of the bridge under different SLR scenarios at 2050 and 2100. As seen, the north side does not experience flooding under any SLR projection in 2050, but it is expected to be inundated by storm surge at year 2100 under IH and extreme SLR scenarios. The extent of flooding is significantly larger in the south side compare to the north side, even at present sea level condition. Figure 7 shows the flood duration and intensity at the James River Bridge. As seen, storm surge flooding at this location occurs only in the IH and extreme conditions at 2100. The flooding time in the south side of the bridge increases linearly with SLR projection for 2050 but increases nonlinearly for 2100. The south side of the bridge starts being flooded since the IL SLR scenario of both 2050 and 2100. This spot is expected to be flooded under extreme SLR without storm surge.

The bridge on I-64 in the City of Chesapeake is the third critical spot to be studied as the flooding around this bridge can affect a substantial traffic

FIGURE 7

Storm surge flooding intensity and duration at north (a, b) and south (c, d) sides of the James River Bridge.

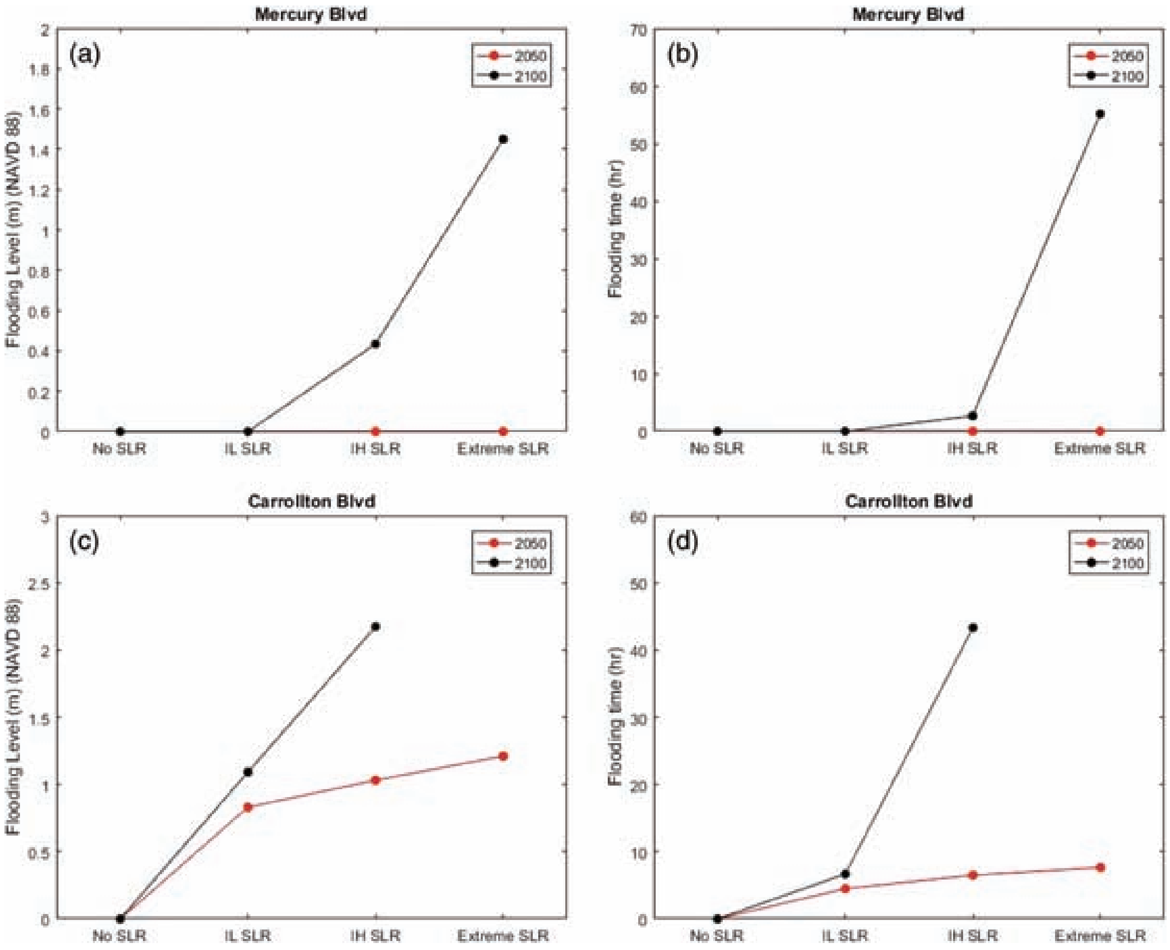

volume. In Figure 8, the extent of storm surge flooding in the east and west sides of the bridge is shown. The storm parameters and SLR projection are the same as those used in the previous simulations. The observation points, which are placed on the road, do not capture any flooding for year 2050, but we note that the east side of the bridge in the vicinity of the river will be flooded even under current sea level. Because of high ground elevation on both sides of the bridge, flooding does not occur at the observation points except in IH and extreme SLR scenarios in 2100 (Figure 9).

To highlight the difference between the hydrodynamic model results and the bathtub approach, we compare the estimates of the two approaches for the IH SLR scenario in the Hague neighborhood of Norfolk. As seen in Figure 10, the bathtub approach overestimates the extent of the flooding, and streets farther from the water front, which will be clear based on the hydrodynamic model results, are expected to be flooded based on the bathtub approach.

FIGURE 8

Flood map at I-64 Bridge in Chesapeake under IL, IH, and extreme SLR in (a) 2050 and (b) 2100.

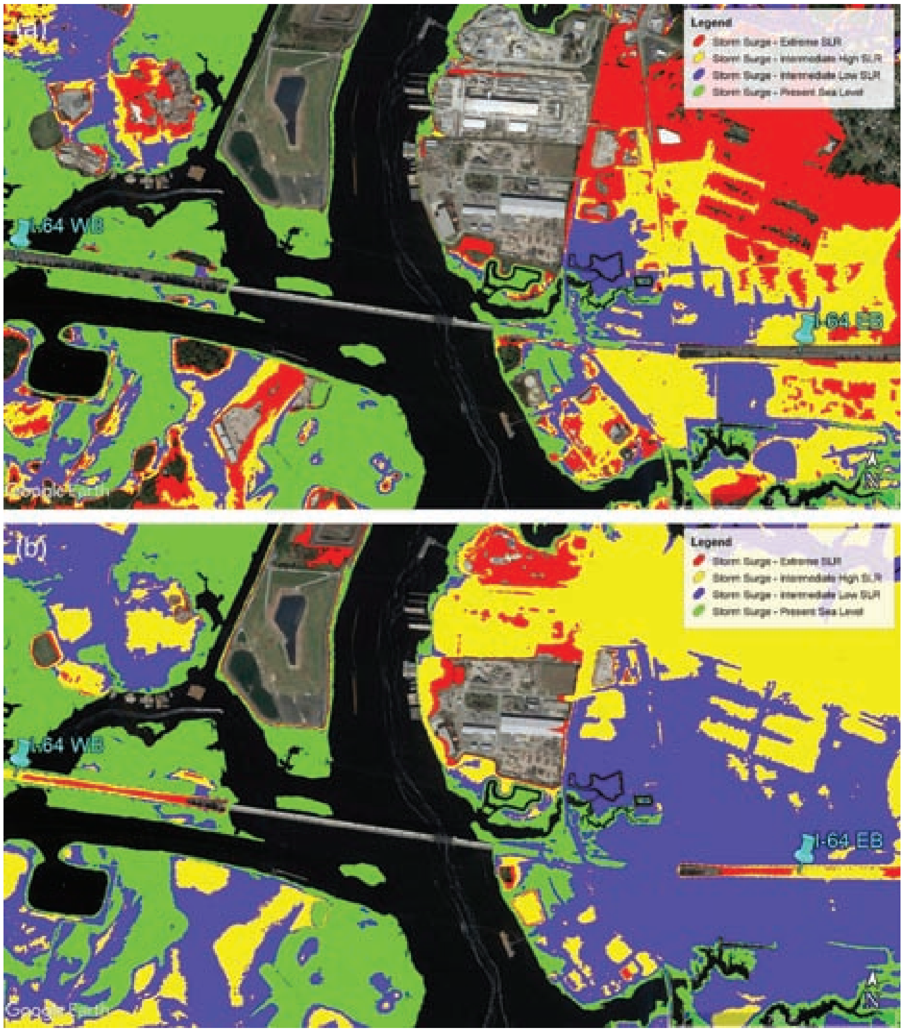

Summary and Discussion

The objective of this research is to improve our understanding of vulnerabilities in the Hampton Roads region of Virginia to storm surge flooding in the face of SLR. In consultation with local and state officials, several critical flood-prone spots were identified. These areas are either in the vicinity of critical emergency facilities or have a substantial traffic flow.

A hydrodynamic model is developed based on the Delft3D modeling suite to simulate storm surge flooding under different SLR conditions. The study focuses on three flood-prone spots representing multiple municipalities in Hampton Roads, namely the cities of Norfolk, Chesapeake, and Newport News and Isle of Wight County. To reduce the computational time, the model was developed at three levels of nesting with spatial resolutions varying from ~200 m to ~2.5 m. The numerical models Level 1, Level 2, and Level 3 used 13, 13, and 59 Intel Xeon E5-2670 v2 2.50 GHz CPUs, respectively. The combined computational time of nested model was between 48 and 72 h, depending on the study site in the Level 3 model.

Three different SLR scenarios, namely IL, IH, and extreme SLR, were selected, and storm surge flood maps were developed for a historic hurricane for the present sea level as well as the projected SLR for 2050 and 2100. The hurricane was defined using the parameters of Hurricane Irene (2011). The first flood-prone areas that are studied are the Hague neighborhood in the City of Norfolk, the James River Bridge connecting

FIGURE 9

Storm surge flooding intensity and duration at west (a, b) and east (c, d) sides of the I-64 Bridge in Chesapeake.

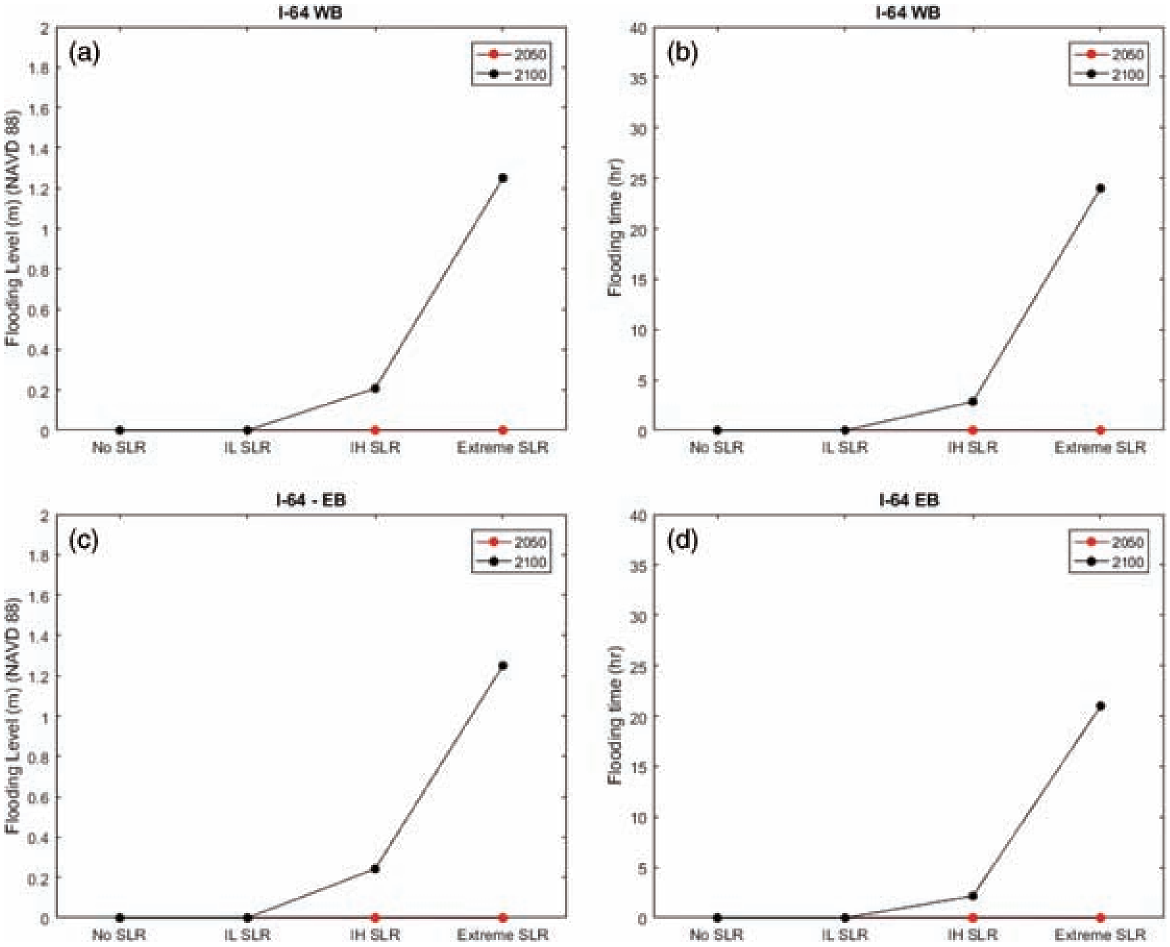

the county of Isle of Wight and the City of Newport News, and the High Rise Bridge over Interstate 64 in the City of Chesapeake. As expected, increase in SLR estimates results in increase in flooding, and the dependency of flooding intensity and duration on SLR are site specific. Tables 3 and 4 summarize the flooding level and duration at these locations, respectively.

We compared the results of the hydrodynamic model for the Hague neighborhood with the widely used bathtub approach for one SLR scenario. The results indicate that the bathtub approach overestimates the extent of the flooding in the selected area; thus, it is critical to use hydrodynamic analysis to estimate SLR impacts on storm surge flooding.

The present study can be improved in several directions. We note that, in a nested modeling approach, all the nested models need to be validated. At the time of our analysis, there was no data available in the domain of models at the third level of nesting. Therefore, although models at the first and second level of nesting were validated with water level data, the information from Level 3 models still requires validation. The City of Norfolk has recently installed a tide gauge in the Hague area, which could be used to validate the Level 3 model and similar hydrodynamic models in the future. The second shortcoming of the study is that the effect of waves is not included. Coupling the spectral wave model SWAN (Booij et al., 1999) with the Delft3D-FLOW model is straightforward in the Delft3D modeling suite and is being conducted in an ongoing study.

Although the present study focuses on three specific spots in the transportation network, the developed model and approach can be applied to other coastal areas vulnerable to storm surge and SLR. The results of this study on the extent, intensity, and duration of flooding under different SLR projections would enable more accurate design and implementation

FIGURE 10

Comparison between the storm surge model estimates for inundation extent under IH SLR in 2050 (yellow) and estimates based on the bathtub approach (red).

of flood mitigation measures such as tide gates, seawalls, or storm water infrastructure and will help the transportation planners and emergency managers with advanced warnings and rerouting of the traffic, thereby increasing the resiliency of the critical infrastructure operations in the region to extreme weather and SLR.

Acknowledgments

The authors thank Kyle Spencer (City of Norfolk) for providing bathymetric and topographic data. Andrew Scott and Robert Morgan (VDOT) and Scott Smith (City of Norfolk) are thanked for useful discussions for identification of flood-prone areas. Discussions with Dr. Mecit Cetin were helpful. This project is funded

TABLE 3

Flood intensity in study areas.

Flooding Level (m)	Current Sea Level	2050 Scenarios			2100 Scenarios		
		IL	IH	Extreme	IH	IL	Extreme
Hague (Fairfax Ave.)	0.26	0.50	0.67	0.85	0.73	1.66	2.66
James River Bridge South (Carrollton Ave.)	0	0.83	1.03	1.21	1.09	2.17	Continues flooding
James River Bridge North (Mercury Ave.)	0	0	0	0	0	0.43	1.45
I-64 West	0	0	0	0	0	0	1.08
I-64 East	0	0	0	0	0	0.41	1.38

TABLE 4

Flood duration in study areas.

Flooding Duration (h)	Current Sea Level	2050 Scenarios			2100 Scenarios		
		IL	IH	Extreme	IH	IL	Extreme
Hague (Fairfax Ave.)	2.17	4.17	5.83	16.83	6.33	42.17	Continues flooding
James River Bridge South (Carrollton Ave.)	0	4.5	6.5	7.67	6.67	43.34	Continues flooding
James River Bridge North (Mercury Ave.)	0	0	0	0	0	2.67	55.17
I-64 West	0	0	0	0	0	0	18
I-64 East	0	0	0	0	0	5	32

by the Virginia Department of Transportation (VDOT) through Virginia Transportation Research Council (VTRC) as part of VDOT's cost-share in support of MATS-UTC.

Corresponding Author:

Navid Tahvildari
Department of Civil and
Environmental Engineering,
Old Dominion University
135 Kaufman Hall
Norfolk, VA 23529
Email: ntahvild@odu.edu

References

Atkinson, J., McKee Smith, J., & Bender, C. 2013. Sea-level rise effects on storm surge and nearshore waves on the Texas Coast: Influence of landscape and storm characteristics. J Waterw Port Coast. 139(2):98-117. https://doi.org/10.1061/(ASCE)WW.1943-5460.0000187.

Bender, M.A., Knutson, T.R., Tuleya, R.E., Sirutis, J.J., Vecchi, G.A., Garner, S.T., & Held, I.M. 2010. Modeled impact of anthropogenic warming on the frequency of intense Atlantic hurricanes. Science. 327(5964):454-8. https://doi.org/10.1126/science.1180568.

Booij, N., Ris, R.C., & Holthuijsen, L.H. 1999. A third-generation wave model for coastal regions: 1. Model description and validation. J Geophys Res-Oceans. 104:7649-66. https://doi.org/10.1029/98JC0262.

Boon, J.D., Brubaker, J.M., & Forrest, D.R. 2010. Chesapeake Bay land subsidence and sea level change. App Mar Sci Ocean Eng. (Rep. No. 425). Gloucester Point, VA: Va. Inst. of Marine Sci.

Castrucci, L. & Tahvildari, N. 2017. Hydrodynamic Modeling of Storm Surge Flooding in the Transportation Infrastructure in Southeast Virginia. In Proceedings of 2017 MTS/IEEE Oceans Conference, Anchorage, AL.

Casulli, V., & Stelling, G. 2011. Semi-implicit sub-grid modeling of three-dimensional free-surface flows. Int J Numer Methods Fluids. 67:441-9. https://doi.org/10.1002/fld.2361.

Dietrich, J.C., Muhammad, A., Curcic, M., Fathi, A., Dawson, C.N., Chen, S.S., & Luettich, R.A., Jr. 2017. Sensitivity of storm surge predictions to atmospheric forcing during Hurricane Isaac. Journal of Waterway, Port, Coastal, and Ocean Engineering. 144(1): 04017035.

Egbert, G.D., & Erofeeva, S.Y. 2002. Efficient inverse modeling of barotropic ocean tides. J Atmos Oceanic Technol. 19(200):183-204. https://doi.org/10.1175/1520-0426(2002)019<0183:EIMOBO>2.0.CO;2.

Ezer, T., Atkinson, L.P., Corlett, W.B., & Blanco, J.L. 2013. Gulf Stream's induced sea level rise and variability along the US mid-Atlantic coast. J Geophys Res-Oceans. 118(2):685-97.

Ezer, T., & Atkinson, L.P. 2014. Accelerated flooding along the U.S. East Coast: On the impact of sea-level rise, tides, storms, the Gulf Stream, and the North Atlantic Oscillations. Earths Future. 2:362-82. https://doi.org/10.1002/2014EF000252.

Gross, J.M., DeMaria, M., Knaff, J.A., & Sampson, C.R. 2004. A new method for determining tropical cyclone wind forecast probabilities. In Preprints, 26th Conf. on Hurricanes and Tropical Meteorology, Miami, FL. Amer. Meteor. Soc. A (vol. 11).

Holland, G.J., Belanger, J.I., & Fritz, A. 2010. A revised model for radial profiles of hurricane winds. Mon Weather Rev. 138(12):4393-401. https://doi.org/10.1175/2010MWR3317.1.

Hu, K., Chen, Q., & Wang, H. 2015. A numerical study of vegetation impact on reducing storm surge by wetlands in a semi-enclosed estuary. Coast Eng. 95:66-76. https://doi.org/10.1016/j.coastaleng.2014.09.008.

Kleinosky, L.R., Yarnal, B., & Fisher, A. 2007. Vulnerability of Hampton Roads, Virginia to storm-surge flooding and sea-level rise. Nat Hazards. 40(1):43-70. https://doi.org/10.1007/s11069-006-0004-z.

Li, H., Lin, L., & Burks-Cope, K.A. 2013. Modeling of coastal inundation, storm surge, and relative sea-level rise at Naval Station

Norfolk, Norfolk, Virginia, USA. J Coastal Res. 29(1):18-30.

Loftis, J.D., Wang, H.V., DeYoung, R.J., & Ball, W.B. 2016. Using Lidar elevation data to develop a topobathymetric digital elevation model for sub-grid inundation modeling at Langley Research Center. J Coastal Res. 76(Suppl 1):134-48. https://doi.org/10.2112/SI76-012.

Lixion, A.A., & Cangialosi, J. 2011. Tropical Cyclone Report Hurricane Irene (AL092011). National Hurricane Center. Available at: http://www.nhc.noaa.gov/data/tcr/AL092011_Irene.pdf

Murdukhayeva, A., August, P., Bradley, M., LaBash, C., & Shaw, N. 2013. Assessment of inundation risk from sea level rise and storm surge in northeastern coastal national parks. J Coastal Res. 29(6a):1-16. https://doi.org/10.2112/JCOASTRES-D-12-00196.1.

Neelz, S., & Pender, G. 2007. Sub-gird scale parameterisation of 2D hydrodynamic models of inundation in the urban area. Acta Geophys. 55:65-72. https://doi.org/10.2478/s11600-006-0039-2.

Sadler, J.M., Haselden, N., Mellon, K., Hackel, A., Son, V., Mayfield, J., … Goodall, J.L. 2017. Impact of sea-level rise on roadway flooding in the Hampton Roads Region, Virginia. J Infrastruct Syst. 23(4):05017006. https://doi.org/10.1061/(ASCE)IS.1943-555X.0000397.

Sebastian, A.G., Proft, J.M., Dietrich, C., Du, W., Bedient, P.B., & Dawson, C.N. 2014 Characterizing storm surge behavior in Galveston Bay using the SWAN + ADCIRC model. Coast Eng. 88:171-81. https://doi.org/10.1016/j.coastaleng.2014.03.002.

Sweet, W.V., Kopp, R.E., Weaver, C.P., Obeyskera, J., Horton, R.M., Thieler, E.R., & Zervas, C. 2017. Global and regional sea level rise scenarios for the United States. NOAA Technical Report NOS CO-OPS 083. Silver Spring, MD: NOAA.

Vatvani, D., Zweers, N.C., Ormondt, M.V., Smale, A.J., Vries, H.D., & Makin, V.K. 2012. Storm surge and wave simulations in the Gulf of Mexico using a consistent drag relation for atmospheric and storm surge models. Nat Hazard Earth Sys. 12(7):2399-410. https://doi.org/10.5194/nhess-12-2399-2012.

Westerink, J.J., Luettich, R.A., Feyen, J.C., Atkinson, J.H., Dawson, C., Roberts, H.J., & Pourtaheri, H. 2008. A basin to channel scale unstructured grid hurricane storm surge model applied to southern Louisiana. Mon Weather Rev. 136(3):833-64. https://doi.org/10.1175/2007MWR1946.1.

Wilson, S.G., & Fischetti, T.R. 2010. Coastline Population Trends in the United States: 1960 to 2008. P25-1139. U. S. Census. Available at: https://www.census.gov/prod/2010pubs/p25-1139.pdf.